SUPPORTING INFORMATION

Characterization of Structural Changes in Aptamer Films for Controlled Release Nanodevices

M. Belén Serrano-Santos, Eduard Llobet, Veli C. Özalp, Thomas Schäfer

EXPERIMENTAL METHODS

All experiments were carried out in PBS-5M (0.01 M phosphate buffered saline; NaCl-0.138 M; KCl-0.0027 M; pH 7.4; 5 mM $MgCl_2$) buffer at a constant temperature of 23 ± 0.1 ºC. For the acoustic wave-based sensor experiments, biotin functionalized sensors (QSX 339) were purchased from Q-SENSE (Biolin Scientific / Q-Sense AB, Västra Frölunda, Sweden). All QCM-D measurements were performed with a *Q-Sense E1* system (Biolin Scientific / Q-Sense AB, Västra Frölunda, Sweden) at 23 ± 0.1 ºC. DNA oligonucleotides were obtained from IDTDNA (Table 1) and avidin as well as all other chemical from Sigma-Aldrich (Madrid, Spain).

Table 1. The sequences of oligonucleotides used in this study.

ATP-Binding Aptamer Hairpin	5'-CACCTGGGGGAGTATTGCGGAGGAAGGTTCCAGGTG-Bio-3'
ATP-Binding Aptamer	5'-CACCTGGGGGAGTATTGCGGAGGAAGGTT-Bio-3'

Bio: Biotin-C6 modification, **Red:** nucleotides added to create hairpin

Avidin was immobilized on biotin-functionalized quartz sensors by injecting a solution of 100 µg/ml buffer for 30 min at a flow rate of 25 µl/min. Biotinylated aptamers were immobilized on the avidin surface by injecting a solution of 5 µM for 30 min at 25 µl/min. Interaction of aptamers with AMP was performed at a flow rate of 100-150µl/min. For the modeling, simultaneously measured changes in frequency and energy dissipation were obtained at harmonics n=1 (5MHz) to n=13 (65MHz). For data analysis, two, three or four harmonics were considered. Under the assumption that the

avidine-biotinylated ATP-binding aptamer layer formed a homogeneous film on the sensor surface, we assumed a density of 1350 $Kg \cdot m^{-3}$ for the adsorbed layer, a density of 1005 $kg \cdot m^{-3}$ and a viscosity of $1.0 \cdot 10^{-3}$ $Pa \cdot s$ for the binding buffer. Densities of 1200 and 1400 $kg \cdot m^{-3}$ for avidin and biotinylated ATP-binding aptamer layers, respectively, were assumed when two distinct adsorbed layers were accounted for in our modeling. Characterization of the ATP-aptamer hairpin binding were conducted with a single-photon counting spectrofluorimeter (FLS920, Edinburgh Instruments).

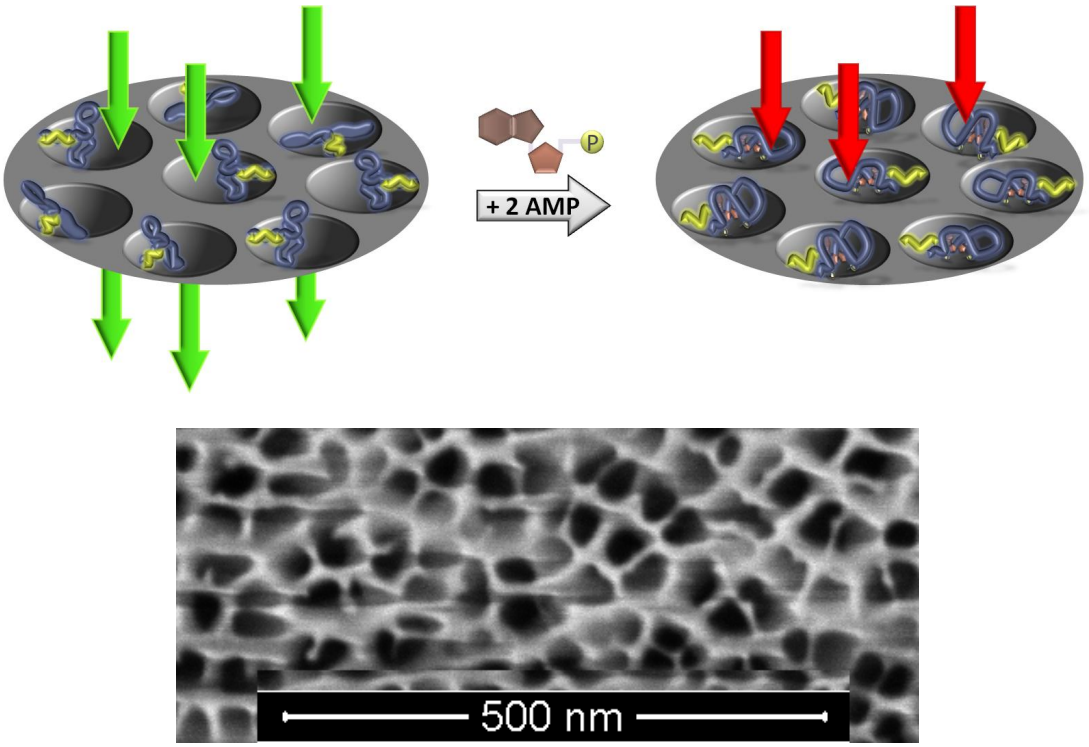

Figure S1. Top: Principle of mesoporous controlled release or gating devices relying on the major conformational changes which DNA aptamers may undergo upon molecular recognition, here as an example an ATP-binding DNA-aptamer. The previously proven concept[15] relies on a major structural change which aptamer or aptamer hairpin structures may undergo upon specifically binding to a molecular target. In this sense, they allow a molecular stimulus to trigger permeability across pores, rather than depending on a bulk stimulus such as pH or temperature, which is a significant advance in designing intelligent nanodevices.

Below: Image taken with Helios NanoLab™ DualBeam™ of mesoporous alumina which can serve as a support structure for gating membranes, prior to surface modification. It can be seen that subsequent modification with aptamers will require knowledge on the expected dimensions of the structural changes such that these devices can be efficient (image courtesy Dr. Andrey Chuvilin, CIC Nanogune, Donostia-San Sebastián, Spain).

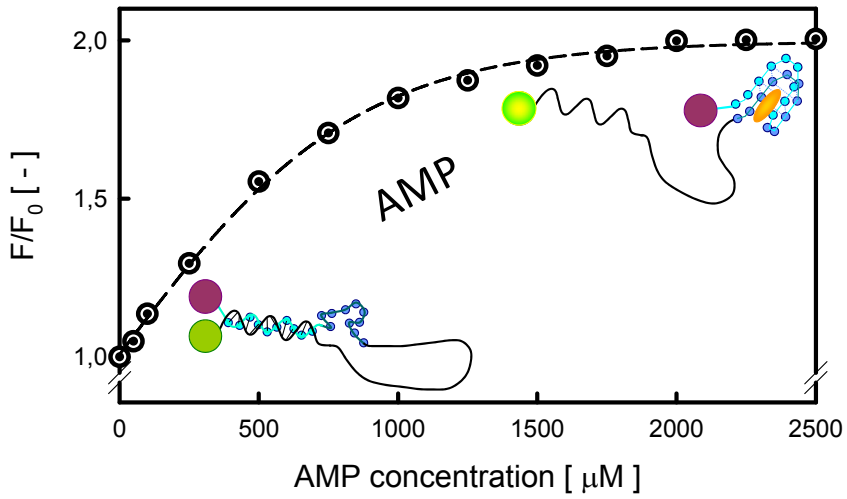

Figure S2. Determination of the dissociation constant K_D of a highly dilute ATP-binding aptamer hairpin structure in solution using single-photon counting spectrofluorimetry and in PBS-5M (0.01 M phosphate buffered saline; NaCl-0.138 M; KCl-0.0027 M; pH 7.4; 5 mM $MgCl_2$) buffer at a constant temperature of 23 ± 0.1 ºC.

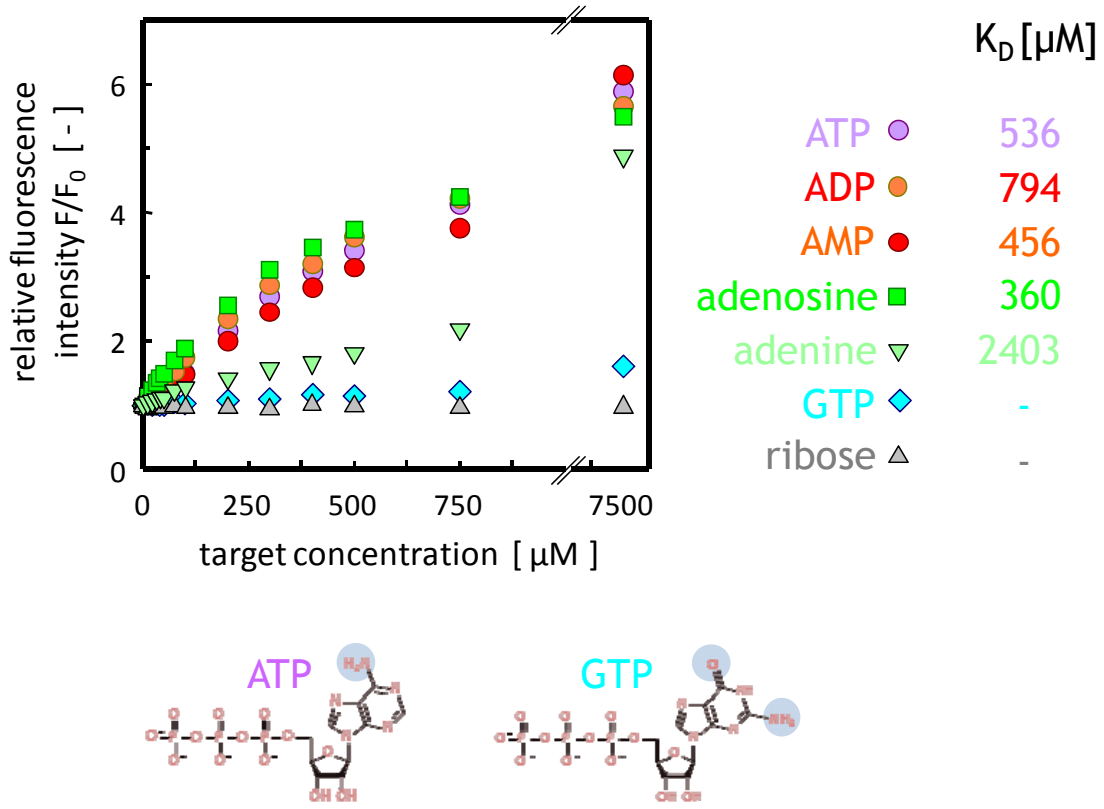

Figure S3. Selectivity of the AMP-aptamer used in this work; according to previous reports[10,19], the aptamer recognizes basically the adenosine part of the target molecule, with the phosphate groups directed away from the binding pocket. This not only explains why the negative charge of the phosphate groups does not interfere with the negative charges on the DNA-aptamer, but also is reflected in the binding constant determined which hardly differ between AMP, ADP and ATP. A minor change in the position and type of functional groups within the recognized part of the target, AMP, results in a clear non-response of the aptamer (example: GTP), illustrating the very high selectivity of the aptamer. Depending on the specific application, obviously the lack of discrimination between AMP, ADP, and ATP might be seen as disadvantageous; however, it should be pointed out that the specificity must be judged with regard to the recognized part of the target molecule (adenosine) and not the parts that in fact do not contribute to the recognition (phosphates). For the latter case, certainly a different kind of aptamer would have to be selected. We have shown that GTP and ATP (or AMP) do indeed trigger opposite responses in DNA-based nanodevices[4].

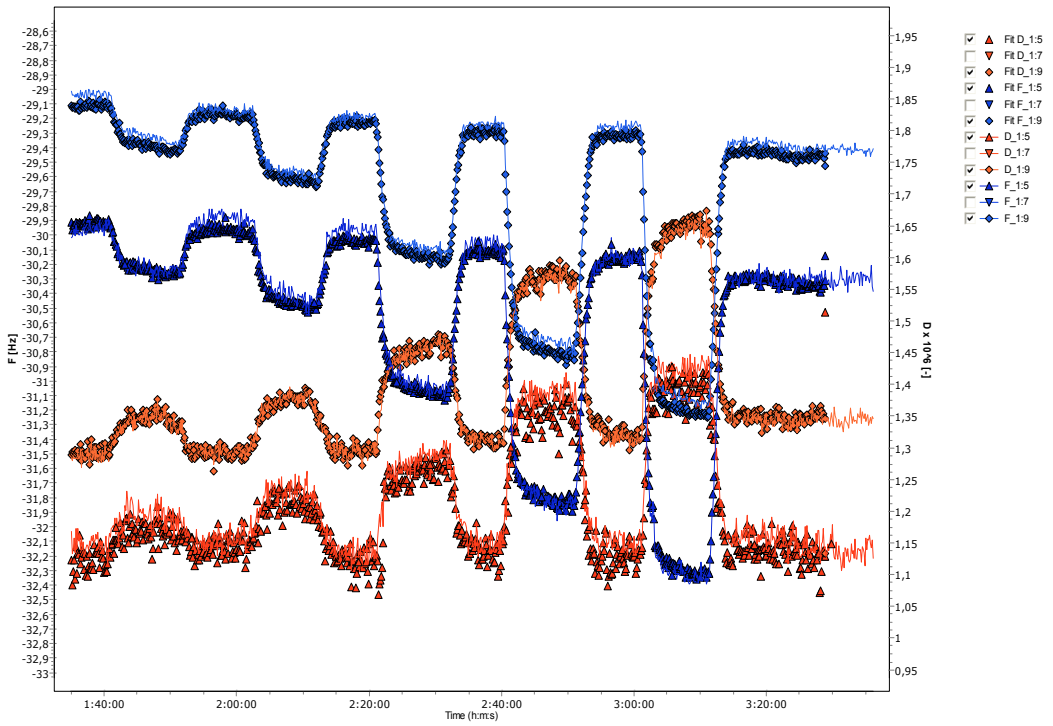

Figure S4. Raw data and corresponding best-fits obtained from two harmonics for frequency (blue lines) and dissipation (red lines) changes during binding of AMP to the ATP-binding aptamer hairpin. Given the subtle changes to be observed during the measurements, it was found crucial to obtain a very good agreement between the data Voigt-based viscoelastic model which is demonstrated in this Figure. Data shown are ΔF (blue lines and symbols) and ΔD (red lines and symbols) versus time at n=5 (triangles) and n=9 (diamonds) overtones for the QCM-D raw data obtained during exposure of the sensor surface to AMP in binding buffer at a series of concentrations (10 up to 750 μM) and corresponding fitting. For clarity, raw data (lines) and corresponding fits (symbols) of only two of the four harmonics used for data processing are depicted. In order to fit our data, we assumed that the density of the buffer and the density of the adsorbed layer were 1005 and 1350 $kg \cdot m^{-3}$, respectively, and two or more harmonics were always considered to estimate the thickness, shear modulus (μ), and shear viscosity (η) of the adsorbed layer. The modeling revealed that the observed increase in layer thickness at increasing concentrations of AMP was accompanied by a progressive decrease in shear viscosity and shear modulus in both structures. However, while in the case of the aptamer film the calculated shear viscosity and shear modulus decreased at an AMP concentration of 750 μM, compared to buffer solution without

target, from $2.3 \cdot 10^{-3}$ to $2.2 \cdot 10^{-3}$ Pa·s and from $6.4 \cdot 10^{5}$ to $5.9 \cdot 10^{5}$ Pa, respectively, in the case of the hairpin structure we determined a decrease of shear viscosity from $1.3 \cdot 10^{-3}$ to $1.2 \cdot 10^{-3}$ Pa·s while the shear modulus decreased from $3.2 \cdot 10^{3}$ to $2.5 \cdot 10^{3}$ Pa for the same concentration of AMP. The observed lower values obtained for the viscoelastic components of the aptamer-hairpin support the above given interpretation of a resulting less compact (or "softer") and less stiff film when interacting with AMP molecules, but most importantly they are in the same range of magnitude as viscoelastic parameters reported previously for DNA hybridization[8].